Evolution of ground state and upper critical field in $R_{1-x}Gd_xNi_2B_2C$ (R=Lu,Y): Coexistence of superconductivity and spin-glass state

S. L. Bud'ko, V. G. Kogan, H. Hodovanets, S. Ran, S. A. Moser, M. J. Lampe, and P. C. Canfield
Ames Laboratory, US DOE and Department of Physics and Astronomy, Iowa State University, Ames, Iowa 50011, USA
(Received 8 September 2010; published 17 November 2010)

We report effects of local magnetic moment, Gd^{3+}, doping ($x \lesssim 0.3$) on superconducting and magnetic properties of the closely related $Lu_{1-x}Gd_xNi_2B_2C$ and $Y_{1-x}Gd_xNi_2B_2C$ series. The superconducting transition temperature decreases and the heat capacity jump associated with it drops rapidly with Gd doping; qualitative changes with doping are also observed in the temperature-dependent upper critical field behavior, and a region of coexistence of superconductivity and spin-glass state is delineated on the x-T phase diagram. The evolution of superconducting properties can be understood within Abrikosov-Gor'kov theory of magnetic impurities in superconductors taking into account the paramagnetic effect on upper critical field with additional contributions particular for the family under study.

DOI: 10.1103/PhysRevB.82.174513 PACS number(s): 74.70.Dd, 74.25.Dw, 74.62.Bf, 75.50.Lk

I. INTRODUCTION

With discoveries of new superconducting materials, classical results on effects of nonmagnetic and magnetic impurities in superconductors[1,2] are being continuously tested and augmented. For example, the searches for impurity-induced states in superconductors[3] and for superconducting quantum critical points[4–6] are few such topics. Unfortunately, in some studies of superconductors with magnetic impurities the emphasis is frequently on just the superconducting properties whereas the state of magnetic subsystem is often neglected.

The rare-earth nickel borocarbides (RNi_2B_2C, R=rare earth) present a rare opportunity to study, within the same family, superconductivity, complex, local moment, magnetism, and their coexistence, as well as physics of strongly correlated, heavy fermion materials.[7–10] In this work we concentrate on thermodynamic and magnetotransport properties of $LuNi_2B_2C$ and YNi_2B_2C superconductors with the nonmagnetic rare earths (Lu or Y) partially substituted by magnetic moment bearing gadolinium. Pure $LuNi_2B_2C$ and YNi_2B_2C have a conveniently high superconducting transition temperatures, T_c, and are readily available as well-characterized single crystals. The details of the superconducting pairing in these materials are still debated with exotic scenarios being examined.[11–15] Since the Gd^{3+} ion has a spherically symmetric, half-filled $4f$ shell, and therefore virtually no crystal electric field effects associated with it, using gadolinium as a magnetic rare-earth dopant may simplify the problem at hand. Although in resistivity and low field dc magnetic susceptibility the features associated with a magnetic subsystem, if located below T_c, are often obscured by strong superconducting signal, it was shown[16–18] that in this situation heat capacity measurements can provide a valuable insight. So far there were several publications, mainly on polycrystalline samples, on physical properties of $Y_{1-x}Gd_xNi_2B_2C$ (Refs. 19–25) and $Lu_{1-x}Gd_xNi_2B_2C$ (Refs. 18, 21, 26, and 27) solid solutions. It is worth noting that although different studies generally agree on the rate of suppression of T_c (on the pure YNi_2B_2C side) and change in the Néel temperature, T_N, (on the pure $GdNi_2B_2C$ side) with x, separation (absence of coexistence) of the superconducting and antiferromagnetic order in $Y_{1-x}Gd_xNi_2B_2C$ near x=0.3 was alluded to in Ref. 25 whereas a coexistence of antiferromagnetism and superconductivity at some region of intermediate concentrations was suggested in Refs. 20 and 23. Additionally, nonmonotonic temperature dependence of the upper critical field, $H_{c2}(T)$, was reported for $Lu_{0.88}Gd_{0.12}Ni_2B_2C$.[27]

A comparative study of the effects of Gd doping on T_c, $H_{c2}(T)$ and the state of magnetic sublattice in $Lu_{1-x}Gd_xNi_2B_2C$ and $Y_{1-x}Gd_xNi_2B_2C$ has the potential to clarify the effect of magnetic impurities on the superconducting state in the rare-earth nickel borocarbides.

II. EXPERIMENT

All samples in this study, $Lu_{1-x}Gd_xNi_2B_2C$ and $Y_{1-x}Gd_xNi_2B_2C$ series, were single crystals, grown using the Ni_2B high temperature growth technique.[7,28,29] *As-grown* crystals were used for this work. Gd concentrations in both series were evaluated through Curie-Weiss fits of the high-temperature part of magnetic susceptibility, that was measured using a Quantum Design, Magnetic Property Measurement System superconducting quantum interference device magnetometer. For resistance measurements a standard, four probe, ac technique (f=16 Hz, I=0.2–2 mA) with the current flowing in the ab plane, close to $I \| a$, was used. For these measurements platinum wires were attached to the samples using EpoTek H20E silver epoxy and the measurements were performed in a Quantum Design, Physical Property Measurement System (PPMS-14) instrument with ac transport (ACT) and He-3 options. $H_{c2}(T)$ data were obtained from temperature-dependent and magnetic field-dependent resistance measurements. For these measurements $H \| c$ direction of the applied field was kept for all samples. Heat-capacity measurements were performed in PPMS-14 instrument with He-3 option utilizing the relaxation technique with fitting of the whole temperature response of the microcalorimeter.

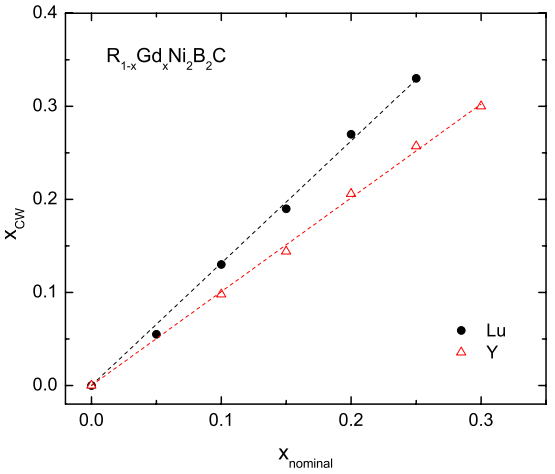

FIG. 1. (Color online) Gd concentration evaluated from a Curie-Weiss fit of the high-temperature susceptibility vs nominal Gd concentration in $R_{1-x}Gd_xNi_2B_2C$, R=Lu, Y. Dashed lines are linear fits with intercept fixed to zero. (See text for details.)

III. RESULTS AND DISCUSSION

A. Heat capacity and *x-T* phase diagram

Since the high-temperature paramagnetism in the $Lu_{1-x}Gd_xNi_2B_2C$ and $Y_{1-x}Gd_xNi_2B_2C$ series is associated only with a local moment bearing Gd^{3+} ion, it was expedient to evaluate the real Gd concentration, x_{CW}, by fitting the measured dc susceptibility $\chi_{dc}=M/H$ (between ~150 K and room temperature) with $\chi_{dc}=x_{CW}C/(T-\Theta)$, where Θ is the Curie-Weiss temperature, $C=(N_A p_{eff}^2)/3k_B$, N_A is the Avogadro number, k_B is the Boltzmann constant, and p_{eff} is the effective moment (for Gd^{3+} $p_{eff}\approx 7.94$ μ_B). Figure 1 shows experimentally evaluated Gd concentration, x_{CW} as a function of the nominal concentration, $x_{nominal}$. For $Y_{1-x}Gd_xNi_2B_2C$ both concentrations are very close to each other $[x_{CW}/x_{nominal}=1.01(1)]$ whereas the difference is fairly large in the case of $Lu_{1-x}Gd_xNi_2B_2C$ $[x_{CW}/x_{nominal}=1.31(2)]$; in both cases the dependence is close to linear in the range of concentrations studied. In the rest of the text, the experimentally determined Gd concentration will be used.

Normalized, zero field, temperature-dependent resistivity data, $\rho(T)/\rho_{300\ K}$, for the $Lu_{1-x}Gd_xNi_2B_2C$ and $Y_{1-x}Gd_xNi_2B_2C$ series are shown in Figs. 2(a) and 2(b). With Gd doping the residual resistivity ratio, RRR=$\rho_{300\ K}/\rho_n$,

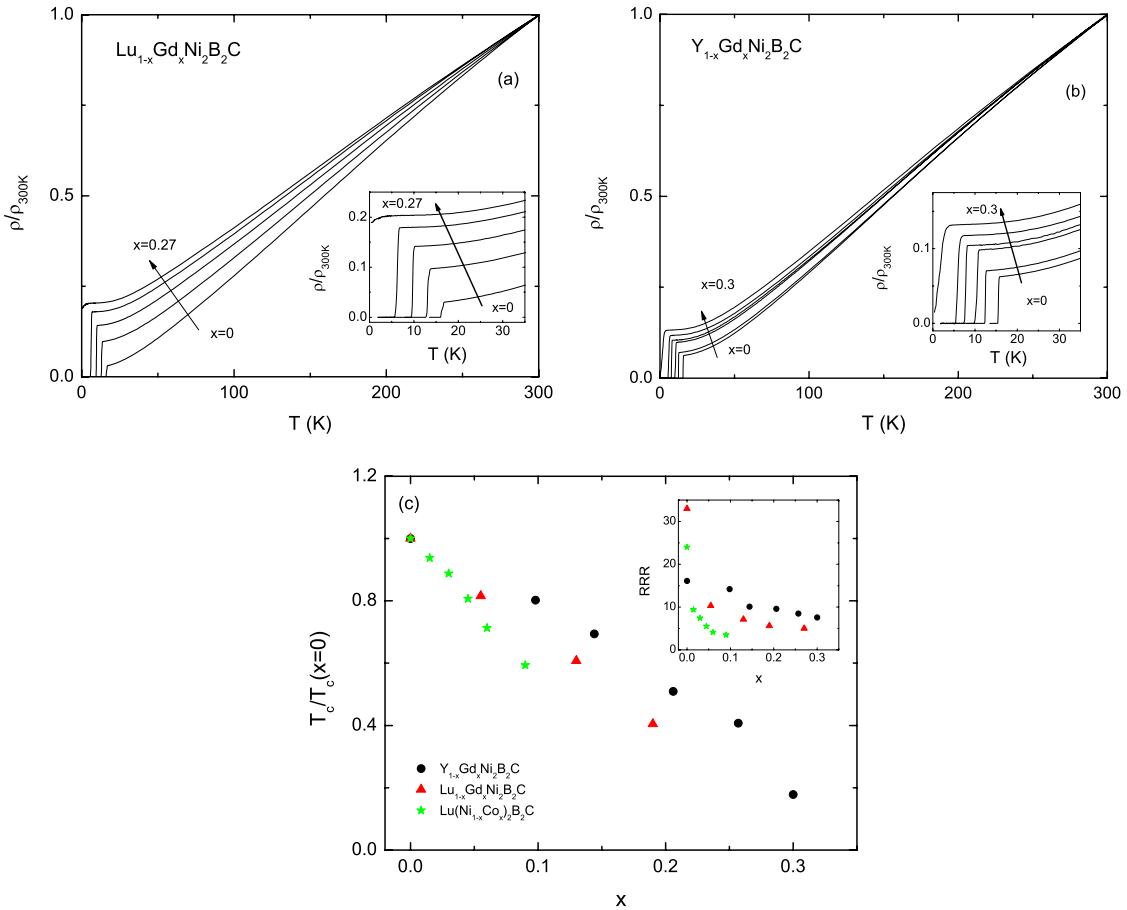

FIG. 2. (Color online) Normalized resistivity, $\rho/\rho_{300\ K}$ for (a) $Lu_{1-x}Gd_xNi_2B_2C$ (x=0, 0.055, 0.13, 0.19, 0.27) and (b) $Y_{1-x}Gd_xNi_2B_2C$ (x=0, 0.10, 0.14, 0.21, 0.26, 0.30). Arrows show the direction of increasing x, insets: low-temperature part of the data. Panel (c): normalized (to the values for the parent compounds) T_c as a function of Gd concentration x for $R_{1-x}Gd_xNi_2B_2C$, R=Lu, Y; data for $Lu(Ni_{1-x}Co_x)_2B_2C$ from Ref. 34 are included for comparison. Inset: RRR vs x for the same three series.

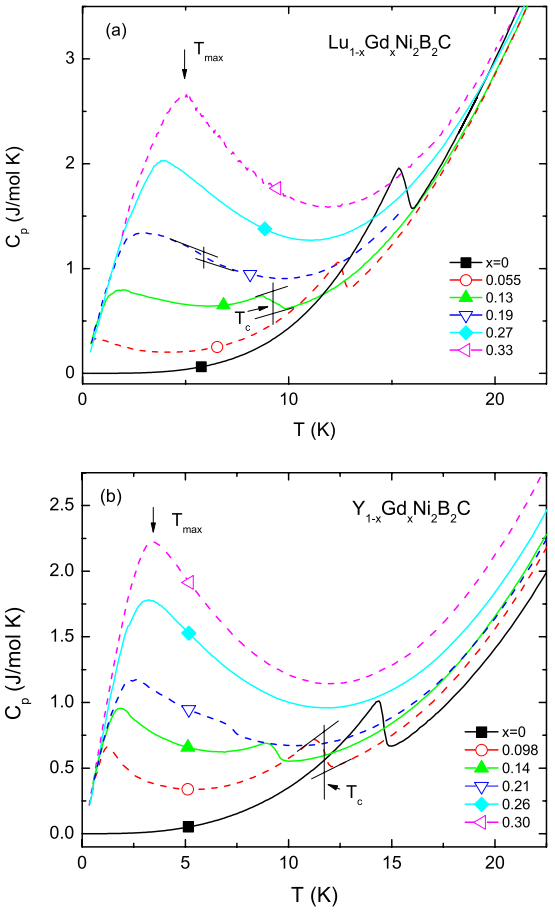

FIG. 3. (Color online) Temperature-dependent heat capacity for (a) $Lu_{1-x}Gd_xNi_2B_2C$ (x=0,0.055,0.13,0.19,0.27,0.33) and (b) $Y_{1-x}Gd_xNi_2B_2C$ (x=0,0.10,0.14,0.21,0.26,0.30). Arrows show examples of how T_{max} and T_c are determined.

where ρ_n is the normal-state resistivity just above the superconducting transition, decreases and the superconducting transition temperature, T_c, decreases as well [Fig. 2(c), inset]. The superconducting critical temperature determined from the onset of the resistive superconducting transition for $Lu_{1-x}Gd_xNi_2B_2C$ and $Y_{1-x}Gd_xNi_2B_2C$ is plotted as a function of Gd concentration in Fig. 2(c). The $T_c(x)$ dependence is close to linear with a downturn seen in the case of $Y_{1-x}Gd_xNi_2B_2C$ for the highest presented doping level. This behavior is consistent with Abrikosov-Gor'kov (AG) theory of pair breaking on magnetic impurities.[2] The rate of T_c suppression is similar for two $R_{1-x}Gd_xNi_2B_2C$ series, being slightly higher for R=Lu. This difference is probably due to the additional contribution of the effect of nonmagnetic scattering in superconductors with anisotropic gap.[30–33] Indeed, RRR (that can be, by Matthiessen's rule, roughly taken as a caliper of scattering, with lower RRR corresponding to higher scattering) decreases with Gd doping faster in the case of R=Lu [Fig. 2(c), inset], that is consistent with larger lattice mismatch (causing stronger scattering) for the Gd/Lu (in comparison to Gd/Y) substitution. For comparison, the data for $T_c(x)$ evolution in $Lu(Ni_{1-x}Co_x)_2B_2C$ from Ref. 34 are included in the same plot. It is worth noting that the T_c suppression rate is higher for Co doping to the Ni site than for

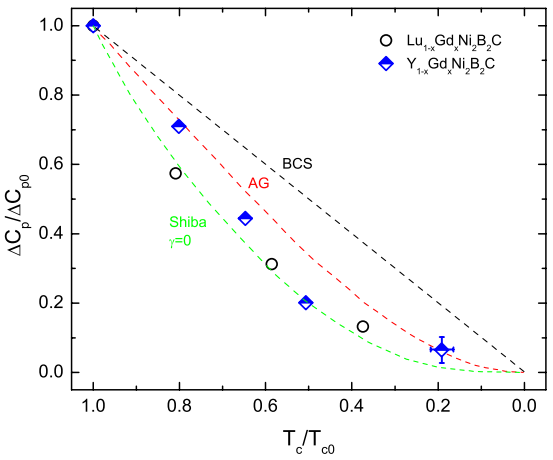

FIG. 4. (Color online) Normalized jump in heat capacity at T_c vs normalized T_c for the $Lu_{1-x}Gd_xNi_2B_2C$ and $Y_{1-x}Gd_xNi_2B_2C$ series (for pure $LuNi_2B_2C$ and YNi_2B_2C ΔC_p at T_c values are 665 mJ/mol K and 460 mJ/mol K, respectively). Dashed lines correspond to BCS law of corresponding states, Abrikosov-Gor'kov magnetic scattering and γ=0 (strong spin-dependent scattering) limit of Shiba's theory (Ref. 43). See text for more details.

Gd doping to the Lu(Y) site, even though among local moment rare-earth (e.g., excluding Ce and Yb) Gd^{3+} (and Eu^{2+}) has the highest de Gennes factor, $(g_J-1)^2J(J+1)$, and the strongest T_c suppression rate.[7,10] The reason for such a strong effect of Co substitution on T_c is at least twofold: first, Co substitution for Ni is not isoelectronic, it induces changes in the density of states at the Fermi level, therefore causing changes in T_c;[35–37] second, for similar concentrations, x, scattering appears to be stronger for Co substitution [Fig. 2(c), inset], thus adding to the T_c suppressing rate.

Zero field, temperature-dependent heat capacity, $C_p(T)$, was measured for the $Lu_{1-x}Gd_xNi_2B_2C$ and $Y_{1-x}Gd_xNi_2B_2C$ series in order to get additional insight into the evolution of the magnetic properties with Gd doping. The results are presented in Fig. 3. For the parent compounds, and several lower Gd concentrations in each series, a jump in $C_p(T)$, at the superconducting transition temperature is clearly seen. This jump broadens with Gd doping thus the value of ΔC_p at T_c was evaluated by the isoentropic construct. Figure 4 shows the heat capacity jump inferred from the isoentropic construct for the $Lu_{1-x}Gd_xNi_2B_2C$ and $Y_{1-x}Gd_xNi_2B_2C$ series normalized to the value of the jump for the parent compounds, $LuNi_2B_2C$ and YNi_2B_2C, respectively, plotted as a function of normalized superconducting transition temperature, T_c/T_{c0}. As expected, the experimental points lay below the BCS law of corresponding states line,[38,39] however, these points also appear to be below the line obtained within the AG theory of pair breaking from magnetic impurities[40] as well. Similar behavior of $\Delta C_p/\Delta C_{p0}$ vs T_c/T_{c0} was observed decades ago for Kondo impurities (with temperature-dependent pair breaking) in superconductors.[41,42] In our case the dopant, Gd^{3+}, is a good local magnetic moment ion for which hybridization and Kondo-related physics are not expected. There are several possible explanations of such behavior that do not invoke the Kondo effect. Qualitatively similar behavior (approximated by $\Delta C_p \propto T_c^2$) was observed

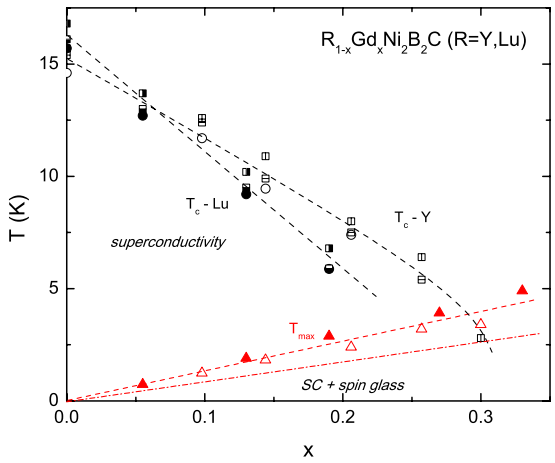

FIG. 5. (Color online) *T*-*x* phase diagram for the $Lu_{1-x}Gd_xNi_2B_2C$ (filled and partially filled symbols) and $Y_{1-x}Gd_xNi_2B_2C$ (open symbols) series. Symbols: squares T_c from onset and offset of the resistive transitions; circles—T_c from heat capacity; triangles—T_{max} from heat capacity. Dashed lines are guides for the eyes. Dotted-dashed line approximates spin-glass phase (crossover) line.

in $Y_{1-x}R_xNi_2B_2C$ (R=Gd, Dy, Ho, and Er)[23] and was attributed to a combination of weak-coupling results of magnetic pair-breaking AG theory with strong-coupling corrections. Alternatively, a Hartree-Fock approach by Shiba[43] yields a band of possible $\Delta C_p/\Delta C_{p0}$ vs T_c/T_{c0} values that is defined within this approach by the value of the parameter γ, related to the strength of spin-flip scattering. For $\gamma \to 1$ (weak scattering) the AG results reproduced. The limit of $\gamma \to 0$ describes strong spin-dependent scattering. Our experimental data lay close to this $\gamma \to 0$ limit (Fig. 4). Another possible explanation may be a combined effect of magnetic and nonmagnetic scattering[44] with a notion that the gap parameter in borocarbides is anisotropic. This last possibility is appealing but requires more theoretical work due to complexity of the theoretical results and a number of independent parameters required for a realistic description.

Our previous data on the $Yb_{1-x}Gd_xNi_2B_2C$ and $Lu_{1-x}Gd_xNi_2B_2C$ series[18] provide experimental evidence that for Gd concentration $x \lesssim 0.3$ the long-range magnetic order observed in pure $GdNi_2B_2C$ and the high Gd end of the series, evolves into a spin glass (SG). A broad maximum in heat capacity marked as T_{max} in Fig. 3 is associated with a spin-glass transition, with $T_{max} \approx 1.5T_f$, for Ruderman-Kittel-

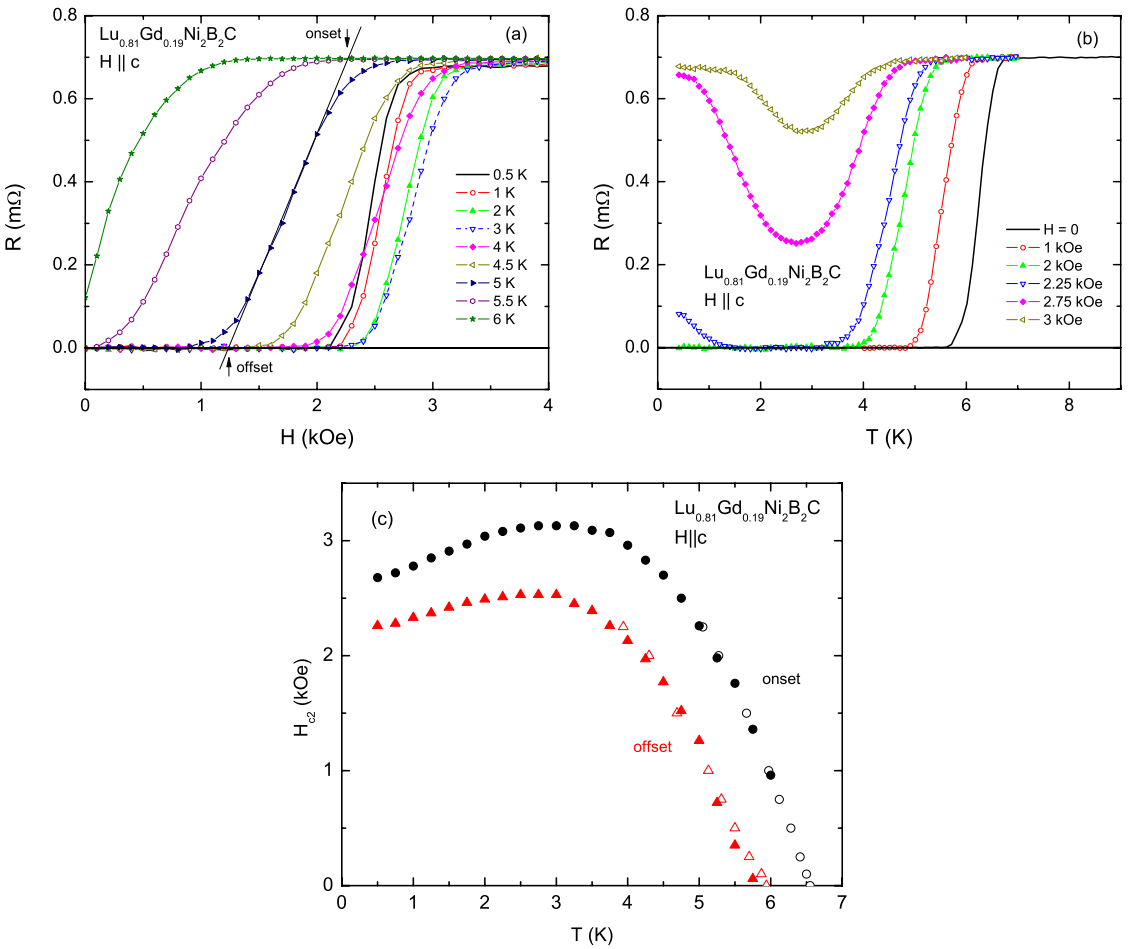

FIG. 6. (Color online) (a) Examples of magnetic field-dependent resistance of $Lu_{0.81}Gd_{0.19}Ni_2B_2C$ single crystal measured at several constant temperatures for $H \| c$. Onset and offset criteria of superconducting transition are illustrated. (b) Examples of temperature-dependent resistance of the same sample measured in different applied magnetic fields. (c) Temperature-dependent upper critical field of $Lu_{0.81}Gd_{0.19}Ni_2B_2C$ for $H \| c$. Circles—onset, triangles—offset, open symbols are from $R(T)|_H$ scans, filled symbols are from $R(H)|_T$ scans.

Kasuya-Yoshida spin glasses,[45] where T_f is the spin-glass freezing temperature.

The other feature in temperature-dependent heat-capacity data (Fig. 3) is a broad minimum. This minimum exists for all of our $x>0$ data and is most probably just a crossover between the low-temperature magnetism-dominated behavior and high-temperature behavior dominated by electron and phonon contributions.

Resistivity and heat-capacity data together allow us to construct the x-T phase diagram for the $Lu_{1-x}Gd_xNi_2B_2C$ and $Y_{1-x}Gd_xNi_2B_2C$ series (Fig. 5). As mentioned above, there is a slight difference in T_c variation with x between R=Lu and R=Y. The other salient temperature, T_{max}, has very similar x dependence in both cases. It has to be mentioned that probing magnetic signatures at temperatures below superconducting transition often is not a simple task. In electric/thermoelectric and low field magnetic susceptibility measurements the superconducting signal dominates. Magnetic field needed to suppress superconductivity might be large enough to alter fragile, low temperature, magnetic state (as it happens, e.g., in materials with field-induced quantum critical point[46]), or at a minimum, shift the phase line. Zero-field heat-capacity measurements clearly reveal (complex) long-range magnetic order below T_c.[17,47] In the case of spin-glass transition heat capacity does not have clear anomaly at the freezing temperature, T_f, instead a broad maximum is detected at $\approx 1.5T_f$.[45] Having this in mind, we can approximately outline (by the dotted-dashed line in Fig. 5) the boundary of the spin-glass phase. Since, at least in zero field resistivity, that was measured in this work down to the temperatures below the SG line for several Gd concentrations, no re-entrance behavior is observed, superconductivity coexists with the SG state at low temperatures. For slightly higher Gd concentrations, after superconductivity is just suppressed, [as it was mentioned for $Lu_{1-x}Gd_xNi_2B_2C$ (Ref. 18)] spin-glass-related behavior is observed both in heat capacity and magnetic susceptibility. On further Gd doping, a long-range magnetic order is established.

B. Upper critical field

The upper critical field was measured resistively, combining magnetic field-dependent data taken at constant temperature and temperature-dependent data taken in fixed magnetic field. Examples of such data for $Lu_{0.81}Gd_{0.19}Ni_2B_2C$ ($H\|c$) are shown in Figs. 6(a) and 6(b). Re-entrant $R(T)$ curves for a few, relatively high, values of magnetic field [Fig. 6(b)] are worth noting. Results obtained from both data sets are consistent, the resulting $H_{c2}(T)$ curves for two different criteria are shown in Fig. 6(c). The aforementioned re-entrant $R(T)$ curves are the results of the horizontal (H=constant) cuts through the shallow maximum in the $H_{c2}(T)$.

The $H_{c2}(T)$ data for the $Lu_{1-x}Gd_xNi_2B_2C$ and $Y_{1-x}Gd_xNi_2B_2C$ series are presented in Fig. 7. The evolution of the upper critical field behavior with Gd doping is similar for both series: the behavior changes from monotonic with temperature for the parent and lightly doped compounds to the behavior with shallow maximum for higher Gd concentrations. This evolution is seen better yet when plotted in

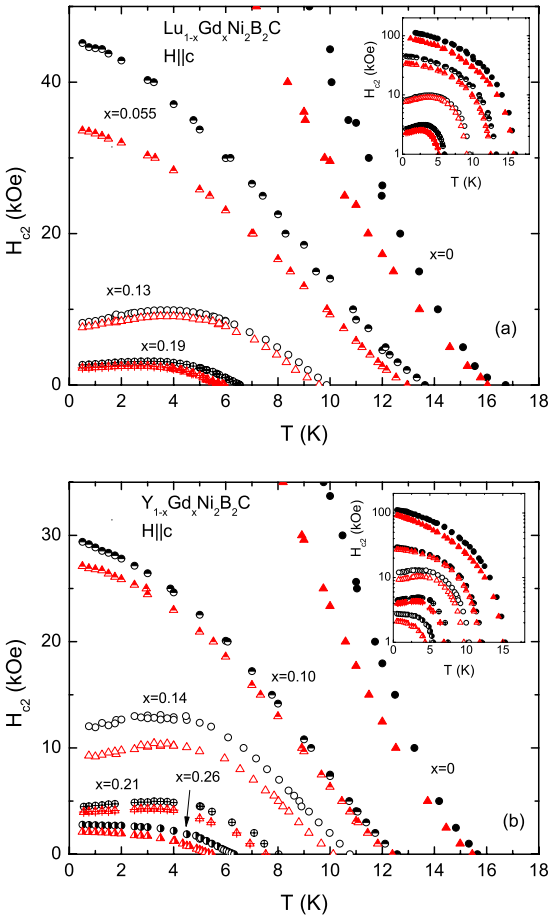

FIG. 7. (Color online) Temperature-dependent upper critical field ($H\|c$) for (a) $Lu_{1-x}Gd_xNi_2B_2C$ (x=0,0.055,0.13,0.19) and (b) $Y_{1-x}Gd_xNi_2B_2C$ (x=0,0.10,0.14,0.21,0.26). Circles and triangles correspond to the onset and offset criteria, respectively. Insets show the same data on a semilog scale.

normalized coordinates (Fig. 8). Qualitatively similar evolution of $H_{c2}(T)$ was theoretically described (in dirty limit) by taking into account paramagnetic effect.[48,49] The use of dirty limit for this materials is consistent with previous studies.[34] The quantitative description of $H_{c2}(T)$ within a paramagnetic effect approach requires detailed knowledge of the paramagnetic contribution to susceptibility below T_c, which is a tedious task. On careful examination of Fig. 8(b) we can see that a noticeable broad maximum in $H_{c2}(T)$ is observed for x=0.14 and x=0.21, however, this maximum practically disappears for the next concentration, x=0.26, for which $H_{c2}(T)$ is monotonic with a tendency to saturation below $T/T_c \approx 0.5$. For this concentration (at zero field) the T_c value is close to T_f, the SG freezing temperature (Fig. 5). For spin glasses the paramagnetic component of susceptibility decreases below T_f (Ref. 45) so that H_{c2} suppression is expected to be weaker, in agreement with our observation. Similar arguments were used in Ref. 50 for interpretation of $H_{c2}(T)$ data below the Néel temperature.

Figure 9 presents the slope of the $H_{c2}(T)$ in the limit of $H\to 0$ as a function of T_c in zero field for the $Lu_{1-x}Gd_xNi_2B_2C$ and $Y_{1-x}Gd_xNi_2B_2C$ series. The observed behavior can be roughly approximated as $dH_{c2}/dT \propto T_c$. It is

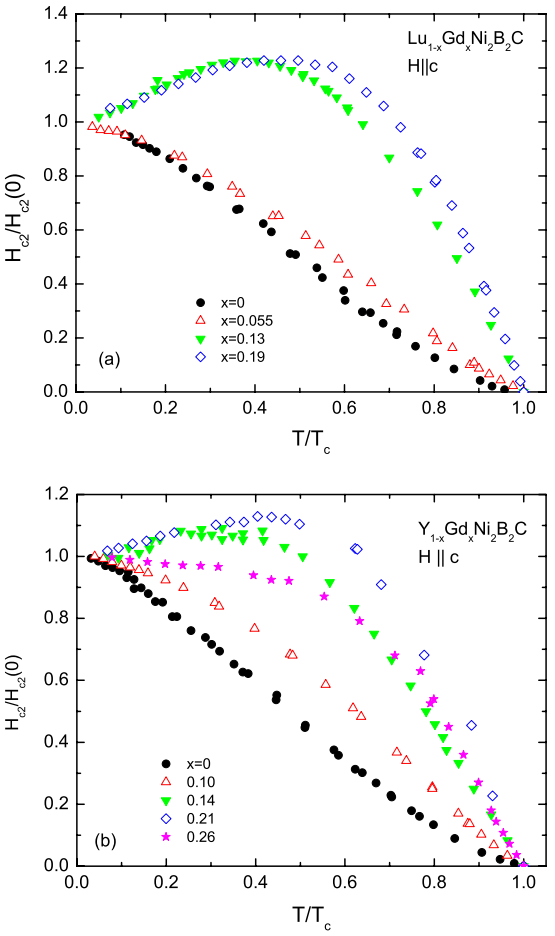

FIG. 8. (Color online) Normalized to $H_{c2}(T=0)$ temperature-dependent upper critical field for (a) $Lu_{1-x}Gd_xNi_2B_2C$ ($x=0$, 0.055, 0.13, 0.19) and (b) $Y_{1-x}Gd_xNi_2B_2C$ ($x=0$, 0.10, 0.14, 0.21, 0.26) as a function of normalized to $T_c(H=0)$ temperature. Data for $H\|c$ obtained using onset criteria are shown.

worth noting that for several recently studied superconductors the behavior is qualitatively different: for $Ce_{1-x}La_xCoIn_5$, dH_{c2}/dT is approximately constant for $H\|c$ and has a factor of two larger absolute value with a slight positive slope for $H\|a$;[51] for neutron-irradiated MgB_2, dH_{c2}/dT is approximately independent of T_c (Ref. 52) whereas for carbon-doped MgB_2, $|dH_{c2}/dT|$ rapidly increases with decrease in T_c (Ref. 53) (opposite to what is observed here); for Co-doped $LuNi_2B_2C$ the derivative decreases in the absolute value only by ≈20% when T_c decreases approximately by half.[34]

It is worth mentioning that $dH_{c2}/dT \propto T_c$ is predicted for isotropic *s*-wave materials in the clean limit. As discussed above, such description appears not to be pertinent to the borocarbides. On the other hand, such proportionality is a property of the AG gapless state[2,33,54] and is present (at least approximately) in the data from elemental La doped with Gd (Ref. 55) (the data in the publication need to be reanalyzed to extract the derivatives). Recently, similar behavior was observed in 1111 family of Fe-As superconductors and was

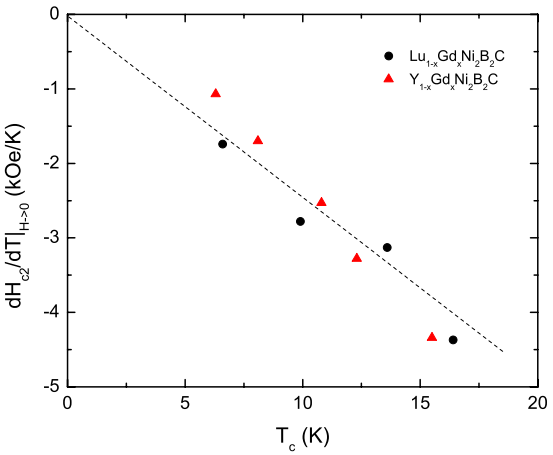

FIG. 9. (Color online) dH_{c2}/dT in the $H\to 0$ limit as a function of T_c in zero field for the $Lu_{1-x}Gd_xNi_2B_2C$ (circles) and $Y_{1-x}Gd_xNi_2B_2C$ (triangles) series. Dashed line is a guide to the eyes.

attributed to pair breaking in anisotropic superconductors.[54]

Following Ref. 54, $|d(dH_{c2}/dT)/dT_c| \propto \pi\phi_0 k_B^2/\hbar^2 v^2$, where ϕ_0 is the flux quantum, k_B is the Boltzmann constant, and v is the Fermi velocity. Since $|d(dH_{c2}/dT)/dT_c| \approx 0.25$ kOe/K^2 (Fig. 9), the order of magnitude estimate gives $v \sim 3\times 10^7$ cm/s. This estimate is consistent with the values used to describe superconductivity in parent $LuNi_2B_2C$ and YNi_2B_2C.[56,57]

IV. SUMMARY

Gd doping of $LuNi_2B_2C$ and YNi_2B_2C results in T_c suppression, consistent with AG magnetic pair breaking with possible additional contribution from nonmagnetic scattering in materials with anisotropic gaps. For both series T_c is suppressed to zero by 30–35 % Gd substitution. The *x*-*T* phase diagram reveals a region of coexistence between superconductivity and a spin-glass state arising from the Gd magnetism. The evolution of the temperature-dependent H_{c2} with Gd doping can be understood by taking into account the paramagnetic effect and for the superconducting sample with highest Gd concentration in this study, $Y_{0.74}Gd_{0.26}Ni_2B_2C$, by considering temperature dependence of paramagnetic susceptibility below the SG freezing temperature. The H_{c2} derivatives in the limit of $H\to 0$ are approximately linear with zero-field superconducting transition temperatures, in agreement with the behavior expected for AG pair breaking.

All in all, the $Lu_{1-x}Gd_xNi_2B_2C$ and $Y_{1-x}Gd_xNi_2B_2C$ series present viable systems for studies of magnetic pair breaking in anisotropic superconductors and interplay of superconductivity and spin-glass state.

ACKNOWLEDGMENT

Work at the Ames Laboratory was supported by the U.S. Department of Energy-Basic Energy Sciences under Contract No. DE-AC02-07CH11358. This manuscript was finalized during the Ames floods of 2010, the second "hundred year floods" in a 15 year time span.

[1] P. W. Anderson, Phys. Rev. Lett. **3**, 325 (1959).
[2] A. A. Abrikosov and L. P. Gor'kov, Zh. Eksp. Teor. Fiz. **39**, 1781 (1960) [Sov. Phys. JETP **12**, 1243 (1961)].
[3] A. V. Balatsky, I. Vekhter, and J.-X. Zhu, Rev. Mod. Phys. **78**, 373 (2006).
[4] R. Ramazashvili and P. Coleman, Phys. Rev. Lett. **79**, 3752 (1997).
[5] V. P. Mineev and M. Sigrist, Phys. Rev. B **63**, 172504 (2001).
[6] N. Shah and A. Lopatin, Phys. Rev. B **76**, 094511 (2007).
[7] P. C. Canfield, P. L. Gammel, and D. J. Bishop, Phys. Today **51**(10), 40 (1998).
[8] K.-H. Müller and V. N. Narozhnyi, Rep. Prog. Phys. **64**, 943 (2001).
[9] K. H. Müller, G. Fuchs, S. L. Drechsler, and V. N. Narozhnyi, in *Handbook of Magnetic Materials*, edited by K. H. J. Buschow (North-Holland, Amsterdam, 2002), Vol. 14, p. 199.
[10] S. L. Bud'ko and P. C. Canfield, C. R. Phys. **7**, 56 (2006).
[11] G. Wang and K. Maki, Phys. Rev. B **58**, 6493 (1998).
[12] K. Maki, P. Thalmeier, and H. Won, Phys. Rev. B **65**, 140502 (2002).
[13] Q. Yuan and P. Thalmeier, Phys. Rev. B **68**, 174501 (2003).
[14] Q. Yuan, H.-Y. Chen, H. Won, S. Lee, K. Maki, P. Thalmeier, and C. S. Ting, Phys. Rev. B **68**, 174510 (2003).
[15] K. Maki, H. Won, and S. Haas, Phys. Rev. B **69**, 012502 (2004).
[16] R. Movshovich, M. F. Hundley, J. D. Thompson, P. C. Canfield, B. K. Cho, and A. V. Chubukov, Physica C **227**, 381 (1994).
[17] R. A. Ribeiro, S. L. Bud'ko, and P. C. Canfield, J. Magn. Magn. Mater. **267**, 216 (2003).
[18] S. L. Bud'ko, J. D. Strand, N. E. Anderson, Jr., R. A. Ribeiro, and P. C. Canfield, Phys. Rev. B **68**, 104417 (2003).
[19] M. E. Massalami, S. L. Bud'ko, B. Giordanengo, M. B. Fontes, J. C. Mondragon, and E. M. Baggio-Saitovitch, Physica C **235-240**, 2563 (1994).
[20] M. El Massalami, S. L. Budko, B. Giordanengo, M. B. Fontes, J. C. Mondragon, E. M. Baggio-Saitovitch, and A. Sulpice, Phys. Status Solidi B **189**, 489 (1995).
[21] P. G. Pagliuso, C. Rettori, S. B. Oseroff, P. C. Canfield, E. M. Baggio-Saitovitch, and D. Sanchez, Phys. Rev. B **57**, 3668 (1998).
[22] M. D. Lan, T. J. Chang, and C. S. Liaw, J. Phys. Chem. Solids **59**, 1285 (1998).
[23] M. El-Hagary, H. Michor, and G. Hilscher, Phys. Rev. B **61**, 11695 (2000).
[24] H. Michor, M. El-Hagary, L. Naber, E. Bauer, and G. Hilscher, Phys. Rev. B **61**, R6487 (2000).
[25] Z. Drzazga, G. Fuchs, A. Handstein, K. Nenkov, and K. H. Müller, Physica C **383**, 421 (2003).
[26] B. K. Cho, P. C. Canfield, and D. C. Johnston, Phys. Rev. Lett. **77**, 163 (1996).
[27] K. D. D. Rathnayaka, D. G. Naugle, A. C. Dumar, M. P. Anatska, and P. C. Canfield, Int. J. Mod. Phys. B **17**, 3493 (2003).
[28] M. Xu, P. C. Canfield, J. E. Ostenson, D. K. Finnemore, B. K. Cho, Z. R. Wang, and D. C. Johnston, Physica C **227**, 321 (1994).
[29] P. C. Canfield and I. R. Fisher, J. Cryst. Growth **225**, 155 (2001).
[30] D. Markowitz and L. P. Kadanoff, Phys. Rev. **131**, 563 (1963).
[31] P. Hohenberg, Zh. Eksp. Teor. Fiz. **45**, 1208 (1963) [Sov. Phys. JETP **18**, 834 (1964)].
[32] L. A. Openov, Pis'ma Zh. Eksp. Teor. Fiz. **66**, 627 (1997) [JETP Lett. **66**, 661 (1997)].
[33] V. G. Kogan, Phys. Rev. B **81**, 184528 (2010).
[34] K. O. Cheon, I. R. Fisher, V. G. Kogan, P. C. Canfield, P. Miranović, and P. L. Gammel, Phys. Rev. B **58**, 6463 (1998).
[35] H. Schmidt, M. Mueller, and H. F. Braun, Physica C **235-240**, 779 (1994).
[36] S. L. Bud'ko, M. Elmassalami, M. B. Fontes, J. Mondragon, W. Vanoni, B. Giordanengo, and E. M. Baggio-Saitovitch, Physica C **243**, 183 (1995).
[37] L. F. Mattheiss, Phys. Rev. B **49**, 13279 (1994).
[38] J. Bardeen, L. N. Cooper, and J. R. Schrieffer, Phys. Rev. **108**, 1175 (1957).
[39] J. C. Swihart, Phys. Rev. **116**, 346 (1959).
[40] S. Skalski, O. Betbeder-Matibet, and P. R. Weiss, Phys. Rev. **136**, A1500 (1964).
[41] E. Müller-Hartmann and J. Zittartz, Solid State Commun. **11**, 401 (1972).
[42] M. Brian Maple, Appl. Phys. **9**, 179 (1976).
[43] H. Shiba, Prog. Theor. Phys. **50**, 50 (1973).
[44] L. A. Openov, Phys. Rev. B **69**, 224516 (2004).
[45] J. A. Mydosh, *Spin Glasses: An Experimental Introduction* (Taylor & Francis, London, 1993).
[46] G. R. Stewart, Rev. Mod. Phys. **73**, 797 (2001); **78**, 743 (2006).
[47] B. K. Cho, P. C. Canfield, L. L. Miller, D. C. Johnston, W. P. Beyermann, and A. Yatskar, Phys. Rev. B **52**, 3684 (1995).
[48] K. Maki, Physics **1**, 127 (1964).
[49] D. Saint-James, G. Sarma, and E. J. Thomas, *Type II Superconductivity* (Pergamon Press, Oxford, 1969).
[50] A. I. Buzdin and L. N. Bulaevskii, Usp. Fiz. Nauk **149**, 45 (1986) [Sov. Phys. Usp. **29**, 412 (1986)].
[51] C. Petrovic, S. L. Bud'ko, V. G. Kogan, and P. C. Canfield, Phys. Rev. B **66**, 054534 (2002).
[52] R. H. T. Wilke, S. L. Bud'ko, P. C. Canfield, J. Farmer, and S. T. Hannahs, Phys. Rev. B **73**, 134512 (2006).
[53] R. H. T. Wilke, S. L. Bud'ko, P. C. Canfield, D. K. Finnemore, R. J. Suplinskas, and S. T. Hannahs, Phys. Rev. Lett. **92**, 217003 (2004).
[54] V. G. Kogan, Phys. Rev. B **80**, 214532 (2009).
[55] P. M. Chaikin and T. W. Mihalishin, Phys. Rev. B **6**, 839 (1972).
[56] V. G. Kogan, M. Bullock, B. Harmon, P. Miranović, Lj. Dobrosavljević-Grujić, P. L. Gammel, and D. J. Bishop, Phys. Rev. B **55**, R8693 (1997).
[57] S. V. Shulga, S.-L. Drechsler, G. Fuchs, K.-H. Müller, K. Winzer, M. Heinecke, and K. Krug, Phys. Rev. Lett. **80**, 1730 (1998).